Chapter 13
Structured Populations

Abstract So far, we have treated populations as homogeneous: all individuals were assumed to be identical with respect to reproduction and dispersal. We only modeled the dynamics of a single density function. In reality, most populations are heterogeneous in many ways. Individuals differ with respect to age, size, gender, and other attributes, and their reproductive and dispersal behavior may depend on these attributes. The nonspatial dynamics of populations with complex life cycles have been successfully described by matrix models. In this chapter, we introduce and study spatially explicit matrix models to generalize the simple IDE to stage-structured populations. We present an in-depth analysis of the critical patch-size problem and the spreading speed for these equations, including several proofs that we omitted in the scalar case in earlier chapters. Throughout the chapter, we use a simple two-stage model for juveniles and adults to illustrate the theory. We close with an overview of the rich literature of applications of structured IDEs to real-world systems, in particular to species invasions.

13.1 Matrix Models

Most populations are heterogeneous in many ways. One of the simplest structures is to distinguish between nonreproductive juveniles and reproductive adults, but many more complex life cycles exist. For example, plant life cycles may include a seed bank, seedlings, and nonflowering and flowering individuals of different sizes and ages. Since reproductive output and dispersal behavior may differ between the different stages, we would like to include this stage-specific information into our models so that we can make accurate predictions. The nonspatial dynamics of such structured populations can be conveniently described by matrix models (Caswell 2001). We briefly review the most important aspects of this theory below. Then we generalize the scalar IDE (2.1) to stage-structured IDEs, or spatially explicit matrix models.

The different stages in the life cycle of an organism can be represented in a life-cycle graph, where vertices represent stages and directed edges indicate possible transitions between stages. For example, if we consider only the two stages of

F. Lutscher, *Integrodifference Equations in Spatial Ecology*, Interdisciplinary Applied Mathematics 49, https://doi.org/10.1007/978-3-030-29294-2_13

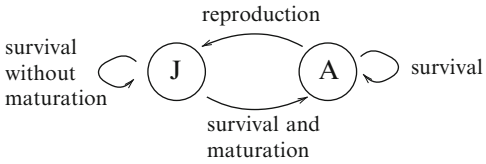

Fig. 13.1 Representation of a simple juvenile–adult two-stage life cycle as a graph.

nonreproductive juveniles and reproducing adults, we need to specify up to four transitions: juveniles remain juveniles if they survive but do not mature, juveniles become adults if they survive and mature, adults remain adults if they survive, and adults produce juveniles; see Fig. 13.1. More generally, structuring populations by age or other relevant life-cycle stages can lead to highly complex life-cycle graphs.

Matrix models are the corresponding mathematical framework for capturing the dynamics of structured populations (Caswell 2001). For example, the juvenile–adult model representing the life-cycle graph in Fig. 13.1 can be written as

$$J_{t+1} = s_j(1-g)J_t + RA_t\,, \qquad A_{t+1} = s_j g J_t + s_a A_t\,, \tag{13.1}$$

where J_t and A_t stand for the number of juveniles and adults in generation t. Parameters s_j and s_a represent the probability of survival of juveniles and adults, respectively; g indicates the probability of maturation; and R is the per capita number of offspring for adults. In general, parameters could depend on population density. This model can be written in matrix notation as

$$\begin{bmatrix} J_{t+1} \\ A_{t+1} \end{bmatrix}_{t+1} = \begin{bmatrix} s_j(1-g) & R \\ s_j g & s_a \end{bmatrix} \begin{bmatrix} J_t \\ A_t \end{bmatrix}. \tag{13.2}$$

More generally, for a population divided into ℓ stages, we denote the number or density of individuals at stage i and generation t by N_t^i, $i = 1, \ldots, \ell$, and the transition (including reproduction) from stage j to stage i by b_{ij}. Then the dynamics between generations can be written as

$$N_{t+1}^i = \sum_{j=1}^{\ell} b_{ij} N_t^j \tag{13.3}$$

or, in matrix notation,

$$\mathbf{N}_{t+1} = B\mathbf{N}_t\,, \quad \text{where} \quad \mathbf{N} = [N^1, \ldots, N^\ell]^T\,, \quad B = [b_{ij}]\,. \tag{13.4}$$

Superscript T stands for the transpose that turns the row vector into a column vector.

When the transition rates between stages are independent of population density, the entries of matrix B are constants and model (13.4) is linear. In that case, we can explicitly solve the recursion by taking powers of B, i.e., $\mathbf{N}_t = B^t\mathbf{N}_0$. To determine the long-term behavior of this solution, we make the important assumption that the

nonnegative matrix B is primitive, i.e., that there is some power of B where all entries are positive (Caswell 2001). The biological meaning of this assumption is that individuals of every stage can be produced from any stage in finitely many time steps. This assumption can be satisfied in many applications by choosing stages appropriately, e.g., by excluding post-reproductive stages. Mathematically, this assumption is the crucial ingredient for proving the Perron–Frobenius theorem; see, e.g., Caswell (2001).

Theorem 13.1 (Perron–Frobenius) *Assume that B is primitive.*[1] *Then B has a simple, positive, strictly dominant eigenvalue with positive eigenvector. No other eigenvalue has a nonnegative eigenvector.*

The fate of the population described by the linear matrix model is completely determined by the dominant eigenvalue, μ, of matrix B. If $\mu < 1$, then the population will go extinct; if $\mu > 1$, then the population will grow indefinitely with asymptotic growth rate μ and the population structure given by the corresponding (right) eigenvector of B.

When the transition rates between stages depend on population density, the elements of $B = B(\mathbf{N})$ depend on the stage vector, and the model is nonlinear. In that case, we find steady states, i.e., solutions of the equation $\mathbf{N}^* = B(\mathbf{N}^*)$; we linearize matrix B at those states; and we determine the stability and bifurcation behavior from the spectrum of the linearization (Caswell 2001; Cushing 2014).

To include space in matrix models, we denote by x the spatial location in some domain of interest, Ω, and by $N_t^i(x)$ the spatial density of individuals at stage i of generation t. Again, we take a census of the population after the end of the dispersal phase. The life cycle begins with the growth phase, which is described by matrix B as above. To model dispersal, we denote by $K_{ij}(x, y)$ the dispersal kernel of individuals at stage i that were produced by individuals at stage j. Then the IDE reads

$$N_{t+1}^i(x) = \int_\Omega \sum_{j=1}^{\ell} K_{ij}(x, y) b_{ij} N_t^j(y) \mathrm{d}y \,. \tag{13.5}$$

With the notation $\bullet$ for the Hadamard product of entrywise matrix multiplication, these equations can be written more elegantly as

[1] The Perron–Frobenius theorem holds under the more general condition that B is *irreducible*. A matrix is irreducible if it is not conjugate to a block upper-triangular matrix (Caswell 2001). A typical example for a reducible matrix arises in populations with post-reproductive stages. Since these stages do not contribute to reproduction, their contribution to the pre-reproductive stages is zero. If we order the variables in the equations such that the post-reproductive stages are first, the resulting matrix will be block upper-triangular. In terms of the life-cycle graph, a matrix is reducible if there is a proper subset of vertices from which there are no edges (transitions) to nodes outside that subset.

$$\mathbf{N}_{t+1}(x) = \int_{\Omega} \mathbf{K}(x, y) \bullet B\mathbf{N}_t(y)\mathrm{d}y\,, \tag{13.6}$$

where $\mathbf{K} = [K_{ij}]$ is the matrix of dispersal kernels.

We analyze these stage-structured IDEs in two steps. We begin with the question of extinction, persistence, and steady states on bounded domains. Then we turn to invasions on unbounded domains.

13.2 Persistence on a Bounded Domain

We begin the analysis of IDE (13.6) on bounded domains. We study steady states and their stability, returning to the question of finding the critical patch-size from Chap. 3 but now for a structured population. This analysis can be seen as generalizing both matrix models to include space and scalar spatial models to include population structure. We present here the more formal underpinnings of the theory that we omitted in Chap. 3. The exposition follows the work by Lutscher and Lewis (2004).

We explicitly denote the dependence of vital rates in matrix B on spatial location and density and write the IDE

$$\mathbf{N}_{t+1}(x) = \mathbf{Q}[\mathbf{N}_t](x) = \int_{\Omega} [\mathbf{K}(x, y) \bullet B(\mathbf{N}_t, y)]\mathbf{N}_t(y)\mathrm{d}y\,, \tag{13.7}$$

where $\Omega \subset \mathbb{R}^n$ is bounded. We work in the product space $\mathscr{L}^2 = (\mathrm{L}^2(\Omega))^\ell$ of square-integrable functions and its positive cone. Accordingly, we make the following assumptions for the rest of this chapter.

(A1) Elements of B are bounded, i.e., $0 \le b_{ij}(\mathbf{N}, y) \le b_{\max} < \infty$ for all i, j. Furthermore, each $b_{ij}(\mathbf{N}, y)$ is continuous with respect to y and continuously differentiable with respect to $\mathbf{N}$.

(A2) If b_{ij} is nonzero, then k_{ij} satisfies $k_{ij} \in (\mathrm{L}^2(\Omega))^2$.

The first assumption is natural for biological populations; it results from even relatively weak self-limitation. Note that we do not assume that the per capita production functions converge to zero. The second assumption requires that all stages disperse. When we allow for sedentary stages, operator Q fails to be compact. We discuss several results on noncompact operators at the end of this chapter.

Lemma 13.1 *Under assumptions (A1)–(A2), operator* $\mathbf{Q} : \mathscr{L}^2 \to \mathscr{L}^2$ *as defined in (13.7) is positive and completely continuous. Furthermore,* $\mathbf{Q}$ *is strongly Fréchet differentiable at* $\mathbf{N} = 0$ *with respect to the positive cone. Its derivative is the positive, completely continuous linear operator given by*

$$\mathbf{Q}'[0]\phi(x) = \int_{\Omega} [\mathbf{K}(x, y) \bullet B(0, y)]\phi(y)\mathrm{d}y\,. \tag{13.8}$$

Proof The proof of this lemma follows from Sects. 17.3, 17.5, and 17.8 as well as Theorem 17.1 in Krasnosel'skii and Zabreiko (1984); see Van Kirk and Lewis (1997) and Lutscher and Lewis (2004). □

The next step is to prove an analogue of the Perron–Frobenius theorem for the linear operator $\mathbf{Q}'[0]$. A linear operator is called *superpositive* (Krasnosel'skii and Zabreiko 1984) if it has a simple positive dominant eigenvalue with positive eigenfunction, and no other eigenfunction is positive. If an operator is superpositive, then the stability of zero and the asymptotic behavior of the equation are determined by the dominant eigenvalue and the corresponding eigenfunction. To show that $\mathbf{Q}'[0]$ is superpositive, we require the following spatial version of primitivity.

(A3) Matrix $B(0, y)$ is primitive for each $y \in \Omega$. Furthermore, if $b_{ij}(0, y)$ is positive for some $y \in \Omega$, then it is positive for all $y \in \Omega$.

In biological terms, these assumptions mean that if individuals at stage j produce individuals at stage i somewhere in the domain, then they do so everywhere, possibly at different rates.

Theorem 13.2 *Assume that (A1)–(A3) hold. In addition, assume that there are constants* $0 < \underline{\kappa} \le k_{ij} \le \overline{\kappa}$ *on* Ω *for all pairs* (i, j) *for which* b_{ij} *is nonzero. Then* $\mathbf{Q}'[0]$ *is superpositive.*

Proof The proof of this theorem follows largely from applying the results from Chap. 2 in Krasnosel'skii (1964). At its core is an application of the Krein–Rutman theorem. The most important estimate is to show that there exists some constant m such that

$$(\underline{\kappa} b_{\min})^m \int \phi(y)\mathrm{d}y \le \mathbf{Q}'[0]^m \phi(x) \le m\ell(\overline{\kappa} b_{\max})^m \int \phi(y)\mathrm{d}y\,. \tag{13.9}$$

This estimate can be obtained in several steps. First, we use primitivity of B to show that if some power of B is positive, then so are all higher powers. Next, we use compactness of the domain to show that some finite power of $B(0, y)$ is positive simultaneously for all y. Finally, we use the lower bounds on the dispersal kernels to obtain the estimate. Then we use the results from Chap. 2 in Krasnosel'skii (1964) together with the properties of the space $\mathscr{L}^2$ to obtain the result; see Lutscher and Lewis (2004). □

The positivity assumption in Theorem 13.2 implies that dispersers can reach any point in the domain from any other point within one dispersal period. This assumption seems unreasonable for some species and certain domains. We relax these assumptions in two steps. First, in the case where Ω is connected, we make the following assumption.

(A4) There is a nonnegative symmetric continuous function κ such that for all $k_{ij} \neq 0$ we have $\kappa(x, y) = \kappa(y, x) \le k_{ij}(x, y) \le \overline{\kappa}$, and there is a constant $\epsilon > 0$ such that for all $x \in \Omega$ the measure of the set $\{y \in \Omega \mid \kappa(x, y) \ge \underline{\kappa} > 0\}$ is at least ϵ.

This assumption covers two important cases. If dispersal distances are small compared to the patch-size, then $k_{ij}(x, y) = 0$ if $|x - y|$ is large. Then the lower bound has to be satisfied for y near x. On the other hand, some dispersal kernels are zero when $x = y$, e.g., the Weibull kernel (see Table 3.1). In that case, the symmetry condition implies that after two dispersal periods, individuals are back near where they started. Hence, the lower bound condition near $x = y$ holds after two dispersal periods.

Proposition 13.1 *Assume that Ω is connected and that (A1)–(A4) hold. Then $\mathbf{Q}'[0]$ is superpositive.*

In the second step, we deal with the case where Ω is a finite collection of disjoint connected components. We write $\Omega = \dot{\bigcup}_{\gamma=1,\dots,\Gamma}\Omega_\gamma$ and assume that each Ω_γ is connected. The *connectivity matrix* $C = (c_{\alpha\beta})$ for continuous kernels k_{ij} is given by

$$c_{\alpha\beta} = \begin{cases} 1, \text{ if for some } \quad x \in \Omega_\alpha, y \in \Omega_\beta, i, j : k_{ij}(x, y)b_{ij}(0, y) > 0\,, \\ 0, \text{ otherwise.} \end{cases} \tag{13.10}$$

Then we need the following assumption.

(A5) Matrix C is primitive.

Assumptions (A4) and (A5) together imply that an individual at stage i and point x can get to any other location $y \in \Omega$ and stage j through dispersal and production in finitely many generations. In mathematical terms, this means that operator $\mathbf{Q}'[0]$ is irreducible.

Proposition 13.2 *Let $\Omega = \dot{\bigcup}_{\gamma=1,\dots,\Gamma}\Omega_\gamma$ be the disjoint union of connected components and assume that (A1)–(A5) hold. Then $\mathbf{Q}'[0]$ is superpositive.*

Proof The proof is tedious but not hard and has a nice biological interpretation. The goal is to prove inequality (13.9). The idea is to find a "connecting path": for any two points x, y in the domain and any two stages i, j in the life cycle, there is a sequence of points in the domain and life stages such that an individual at stage j and location y produces an individual at stage i and location x with positive probability in finitely many generations. Then we use compactness to find the smallest number of generations so that such a sequence exists for all points and life stages. Details are provided in Lutscher and Lewis (2004). □

The theory we have developed so far implies that if the assumptions are satisfied, then the stability of the zero solution is determined by the dominant eigenvalue of the linearized operator at zero; see (13.8). Calculating this dominant eigenvalue for particular examples is a different matter. The calculation can be carried out when all the dispersal kernels are identical Laplace kernels, i.e., when dispersal behavior is independent of stage, and when vital rates are independent of spatial location. In that case, the calculations from Sect. 3.2 can be extended to the stage-structured model. We present this calculation here and give a different example in the next section.

The eigenvalue equation with $B = B(0)$ on the domain $\Omega = [-L/2, L/2]$ is

$$\lambda\phi(x) = \mathbf{Q}'[0]\phi(x) = \int_{-L/2}^{L/2} \frac{a}{2} \exp(-a|x-y|) B\phi(y) \mathrm{d}y \,. \tag{13.11}$$

Differentiating this equality twice and substituting as in Sect. 3.2 leads to the vector-valued boundary-value problem

$$\phi''(x) = -a^2 \left(\frac{1}{\lambda} B - I \right) \phi \,, \qquad \phi'(\pm L/2) \pm a\phi(\pm L/2) = 0 \,, \tag{13.12}$$

where I denotes the identity matrix. The exponential ansatz $\phi(x) = \mathrm{e}^{\xi x}\psi$ leads to the eigenvalue problem

$$\xi^2 \psi = -a^2 \left(\frac{1}{\lambda} B - I \right) \psi \,. \tag{13.13}$$

Hence, we can express ξ via the eigenvalues μ_i of B and the eigenvalue λ of $\mathbf{Q}'[0]$ as

$$\xi^2 = -a^2 \left(\frac{\mu_i}{\lambda} - 1 \right) \,. \tag{13.14}$$

If the expression on the right-hand side is positive, then we get real solutions $\xi = \pm a\sqrt{1-\mu_i/\lambda}$. Since dispersal is symmetric, the eigenfunctions of $\mathbf{Q}'[0]$ have to be symmetric on $[-L/2, L/2]$, which leads to the form

$$\phi(x) = \cosh\left(a\sqrt{1-\mu_i/\lambda}\, x \right) \psi \,. \tag{13.15}$$

These solutions cannot satisfy the boundary conditions. We can rule out $\xi = 0$ equally easily. Therefore, the right-hand side in (13.14) must be negative, which implies $\lambda < \mu_i$. In particular, if the dominant eigenvalue of matrix B is less than unity, then λ is less than unity. In biological terms, if the population goes extinct in the nonspatial setting, then it will also go extinct in the spatial setting. Again, we see that boundary loss reduces the overall population growth rate.

When the right-hand side of (13.14) is negative, we obtain eigenfunctions of the form

$$\phi(x) = \cos\left(a\sqrt{\mu_i/\lambda - 1}\, x \right) \psi \,. \tag{13.16}$$

For the critical patch-size, we set $\lambda = 1$, take the largest eigenvalue of B, and solve as in Sect. 3.2 to get

$$L^* = \frac{2}{a\sqrt{\mu_1 - 1}} \arctan\left(\frac{1}{\sqrt{\mu_1 - 1}} \right) \,. \tag{13.17}$$

From the explicit expression for L^*, we conclude that if matrix B depends on a parameter, say P, and if the dominant eigenvalue is an increasing function of that parameter, then the critical patch-size is a decreasing function of that parameter, i.e., $dL^*(P)/dP < 0$. This relationship actually holds in much more generality when the dispersal behavior of the different stages differs.

Lemma 13.2

1. *On a fixed domain, suppose that the matrix of production rates, $B(0, y; P)$, is nondecreasing in P. Denote $\lambda(P)$ as the dominant eigenvalue of $\mathbf{Q}'[0]$. If at least one entry of $B(0, y; P)$ is strictly increasing in P, then so is $\lambda(P)$.*
2. *Fix P and let $\Omega = [0, L]$. Assume that the matrix of dispersal kernels is of the form $\mathbf{K}(x, y) = \mathbf{K}(x - y) > 0$, and denote $\lambda(L)$ as the dominant eigenvalue of $\mathbf{Q}'[0]$. Then $\lambda(L)$ is a strictly increasing function of L.*
3. *If both previous conditions are satisfied, then $dL^*(P)/dP < 0$.*

The first two statements in the lemma are proved in Lutscher and Lewis (2004). The last statement follows from the implicit function theorem applied at the bifurcation point where $\lambda(L, P) = 1$. In biological terms, this result means that if at least one of the vital rates of the population increases, then the critical patch-size decreases.

13.3 Application

We apply some of the preceding ideas to a three-stage life-cycle model for the common lizard (*Lacerta vivipara*). This example was originally presented by Tricia Morris in her honor's thesis in 2017. The common lizard has three life stages (Galliard et al. 2010). The early juvenile stage (E) lasts for one year. After that year, lizards disperse to find their own territory and enter the late juvenile stage (L), which lasts for another year. At the beginning of their third year, they turn into adults (A) and can continue to live for several years. We denote by $\mathbf{N} = [E, L, A]^T$ the densities of the three stages. We consider linear, space-independent survival probabilities s_X for stage $X \in \{E, L, A\}$ and a linear, space-independent birth term with an average of b (female) offspring per (female) adult. We assume no mating limitation. Then the dynamics between years can be written as

$$\mathbf{N}_{t+1}(x) = \int_\Omega \mathbf{K}(x - y) \bullet B\mathbf{N}_t(y)\mathrm{d}y$$

with

$$\mathbf{K}(x) = \begin{bmatrix} 0 & 0 & \delta(x) \\ K(x) & 0 & 0 \\ 0 & \delta(x) & \delta(x) \end{bmatrix} \quad \text{and} \quad B = \begin{bmatrix} 0 & 0 & b \\ s_E & 0 & 0 \\ 0 & s_L & s_A \end{bmatrix}.$$

Here, K denotes the dispersal kernel at the end of the early juvenile phase. Since only one of the three stages disperses, delta distributions appear at the other stage transitions. The resulting operator is not compact. Condition (A4) on the existence of a simultaneous positive subfunction is also violated. Nonetheless, we can continue with the analysis by a reduction argument.

The corresponding eigenvalue problem is

$$\begin{aligned}
\lambda\phi_1(x) &= b\phi_3(x)\,,\\
\lambda\phi_2(x) &= s_E\int_\Omega K(x-y)\phi_1(y)\mathrm{d}y\,,\\
\lambda\phi_3(x) &= s_L\phi_2(x) + s_A\phi_3(x)\,.
\end{aligned}$$

Substituting the equations for ϕ_1 and ϕ_2 into the third equation, we find

$$\lambda^2\phi_3(x) = s_L s_E b\int_\Omega K(x-y)\phi_3(y)\mathrm{d}y + \lambda^2 s_A\phi_3(x)$$

and eventually

$$\tilde{\lambda}\phi_3(x) = \int_\Omega K(x-y)\phi_3(y)\mathrm{d}y, \quad \tilde{\lambda} = \frac{\lambda^3-\lambda^2 s_A}{s_L s_E b}\,.$$

This integral operator is compact and positive under the usual assumptions on K and Ω. Hence, a dominant eigenvalue $\tilde{\lambda} > 0$ exists. For every $\tilde{\lambda} > 0$, the above condition defines a unique $\lambda > s_A$. The largest value of λ corresponds to the largest value of $\tilde{\lambda}$. In particular, the persistence threshold is given by $\lambda = 1$ or $\tilde{\lambda} = \frac{1-s_A}{s_L s_E b}$.

Since the integral operator contains only dispersal, its dominant eigenvalue is bounded by $\tilde{\lambda} \leq 1$. Hence, we require $b > \frac{1-s_A}{s_E s_L}$ for there to be a solution with $\lambda = 1$. This condition means that each adult has to produce at least one offspring that reaches adulthood for the population to persist. With the survival probabilities estimated at $s_E = 27.9\%$, $s_L = 65.4\%$, and $s_A = 50.6\%$ (Galliard et al. 2010), we require the average number of (female) offspring to be at least $b > 2.7$ for population persistence on a large enough domain. For a given b above this threshold, we can calculate the critical patch-size. If we choose the Laplace kernel with parameter a, we can use the results from Chap. 3 to find the critical patch-size as

$$L^* = \frac{2}{a\sqrt{\frac{s_L s_E b}{1-s_A}-1}}\arctan\left(\frac{1}{a\sqrt{\frac{s_L s_E b}{1-s_A}-1}}\right).$$

With a mean dispersal distance of $a^{-1} = 64.7$ m (Warner and Shine 2008) and $b = 3$, we find a critical patch-size of $L^* = 487.88$ m.

13.4 Nonlinear Analysis

In this section, we present some of the theory that allows us to prove the existence and uniqueness of a positive fixed point. It is based on bifurcation theory and monotone systems theory. We begin with an additional assumption on the vital rates for large population density.

(A6) There is some matrix-valued function $B(\infty, y)$ such that

$$\|B(\mathbf{N}(y), y) - B(\infty, y)\| \leq \frac{\text{const.}}{\|\mathbf{N}\|} \qquad \text{for large} \quad \|\mathbf{N}\| . \tag{13.18}$$

Lemma 13.3 *Assume that (A1), (A2), and (A6) are satisfied. Then, by Sect. 3.2.1 in Krasnosel'skii (1964) and Theorem 17.2 in Krasnosel'skii and Zabreiko (1984), operator* $\mathbf{Q}$ *has a strong asymptotic derivative at infinity. It is given by the completely continuous operator*

$$\mathbf{Q}'[\infty]\phi(x) = \int [\mathbf{K}(x, y) \bullet B(\infty, y)]\phi(y)\mathrm{d}y . \tag{13.19}$$

Proposition 13.3 (Existence of Fixed Points) *Assume that (A1)–(A6) hold. Suppose that the spectral radius of* $\mathbf{Q}'[\infty]$ *is less than one and that the dominant eigenvalue of* $\mathbf{Q}'[0]$ *is greater than one. Then by Theorem 4.11 in Krasnosel'skii (1964), operator* $\mathbf{Q}$ *has a positive fixed point.*

Under additional assumptions about the vital rates, we can even get the uniqueness of the positive fixed point. We have already encountered these conditions in Chap. 4 for unstructured populations. When the population growth function was monotone and concave down, we obtained a unique positive fixed point. The following proposition generalizes this result to structured populations.

Proposition 13.4 (Uniqueness of Fixed Points) *Let the assumptions of Proposition 13.3 be satisfied. Assume in addition that the function*

$$\mathbf{N} \mapsto B(\mathbf{N})\mathbf{N} \tag{13.20}$$

is increasing and that

$$t \mapsto B(t\mathbf{N}) \tag{13.21}$$

is decreasing for $0 \leq t \leq 1$. *Then* $\mathbf{Q}$ *is concave and monotone. By Theorem 6.3 in Krasnosel'skii (1964), the positive fixed point is unique. By Theorem 6.6 in*

Krasnosel'skii (1964), every solution with $\mathbf{N}_0 \neq 0$ *converges to the positive fixed point.*

The concavity condition in the preceding proposition is fairly strong, as we will see in an example below. Weaker conditions are "strict sublinearity" (Zhao 1996) or "strict subhomogeneity" (Zhao 2003). When the concavity conditions are not satisfied, we can still obtain the existence of a (unique) fixed point by studying the behavior near the bifurcation point $\lambda = 1$. In order to apply the theory, we need to exclude the Allee effect; compare Chap. 4. The following assumption is the stage-structured formulation that accomplishes that goal.

(A7) The production rates decrease with population density in any state; i.e., they satisfy $(\partial/\partial N_l)b_{ik} \leq 0$ for all i, k, l, and the inequality is strict for at least one set i, k, l.

We present two forms of the bifurcation results: one with respect to a parameter that affects the vital rates of the population and one with respect to domain length. We denote the parameter by P, the dominant eigenvalue of $\mathbf{Q}'[0]$ by $\lambda = \lambda(P)$, and the bifurcation point by $\lambda(P^*) = 1$. Proofs of both results can be found in Lutscher and Lewis (2004).

Lemma 13.4 (Bifurcation I) *Assume that (A1)–(A7) are satisfied and that the spectral radius of* $\mathbf{Q}'[\infty]$ *is less than one, independent of* P *close to* P^*. *Assume that the production rates* b_{ij} *are nondecreasing in* P *and that at least one of the rates is increasing in* P. *Then there is a transcritical bifurcation at* $P = P^*$*; i.e., a continuous branch of solutions intersects the zero solution. The nonzero solution is positive for* $P > P^*$.

To present a bifurcation result with respect to domain length L, we denote $\lambda(L)$ as the dominant eigenvalue of $\mathbf{Q}'[0]$ and $\lambda(L^*) = 1$ as the bifurcation point. To formulate the result, it is convenient to introduce a generalization of the dispersal success function (see Chap. 9) to the case of structured populations. We define

$$s_{ij}(y) = \int_{\Omega} k_{ij}(x, y)\mathrm{d}x \tag{13.22}$$

as the dispersal success function of an individual at stage i produced from an individual at stage j.

Lemma 13.5 (Bifurcation II) *Assume that (A1)–(A7) are satisfied and that the spectral radius of* $\mathbf{Q}'[\infty]$ *is less than one, independent of* L *close to* L^*. *Assume that the dispersal success functions* s_{ij} *are nondecreasing in* L *and that at least one of them is increasing in* L. *Then there is a transcritical bifurcation at* $L = L^*$*; i.e., a continuous branch of solutions intersects the zero solution. The nonzero solution is positive for* $L > L^*$.

13.5 Example: Juveniles and Adults

We return to the example of a simple population structure of juveniles and adults as in (13.2) and illustrate the conditions of the preceding lemmas and propositions as well as the resulting dynamics. We take advantage of the fact that the nonspatial model was studied in great detail by Neubert and Caswell (2000b) and that most of its dynamic behavior is well understood.

We begin with the scenario that only offspring production is density dependent and replace R with $R(1 + J + A)^{-1}$. Writing $\mathbf{N} = (J, A)^T$, the resulting matrix of vital rates and its limits at zero and infinity are

$$B(\mathbf{N}) = \begin{bmatrix} s_j(1-g) & \frac{R}{1+J+A} \\ s_j g & s_a \end{bmatrix}, \quad B(0) = \begin{bmatrix} s_j(1-g) & R \\ s_j g & s_a \end{bmatrix}, \quad B(\infty) = \begin{bmatrix} s_j(1-g) & 0 \\ s_j g & s_a \end{bmatrix}. \tag{13.23}$$

The dominant eigenvalue, μ_1, of $B(0)$ is an increasing function of R. For $R = 0$, we have $\mu_1 = \max\{s_j(1-g), s_a\} < 1$ and $B(\infty) = B(0)$. When R is large enough, we have $\mu_1 > 1$. The critical value for $\mu_1(R^*) = 1$ is

$$R^* = \frac{(1 - s_a)(1 - s_j(1 - g))}{s_j g}. \tag{13.24}$$

Furthermore, with this choice of density dependence, assumptions (A1), (A3), and (A6), as well as the assumption in Proposition 13.4, are satisfied.

We choose the domain $\Omega = [0, L]$ and let all dispersal kernels be equal to the Laplace kernel with identical variance. Then the remaining assumptions are also satisfied. Therefore, operator $\mathbf{Q}'[0]$ will have a dominant eigenvalue $\lambda = \lambda(R, L)$. If that eigenvalue is less than unity, then the population extinction state will be stable. If it is greater than unity, then there will be a unique, globally stable positive population persistence state. The condition $\lambda(R, L) > 1$ requires $R > R^*$ from (13.24) and $L > L^*$ from (13.17).

A more interesting dynamical scenario arises when density dependence follows the Ricker function; i.e., we replace R in (13.2) with $R \exp(-(J + A))$. This case is studied in detail by Lutscher and Lewis (2004). The resulting matrices, $B(0)$ and $B(\infty)$, are the same as in (13.23), but the monotonicity assumption in Proposition 13.4 is not satisfied. Lemmas 13.4 and 13.5 give the local existence and stability of a positive equilibrium near the bifurcation point. However, increasing parameter R can destabilize the positive steady state and lead to two-cycles and more complicated dynamic behavior. We illustrate some of these behaviors with the simplified model where all stages have the same dispersal behavior, described by the Laplace kernel. Hence, we study the equation

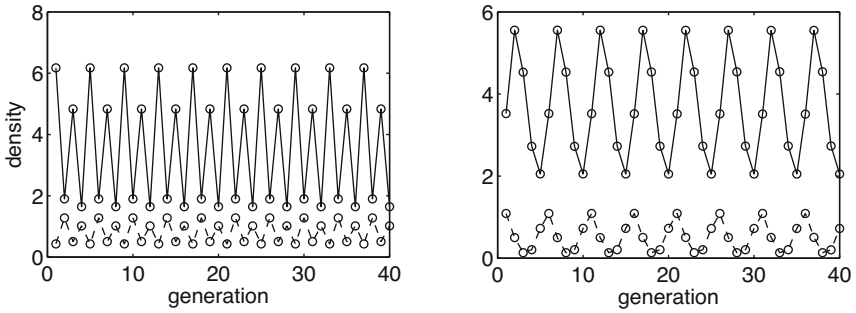

Fig. 13.2 Left: Stable four-cycle in the nonspatial matrix model with Ricker-type density-dependent reproduction ($R = 80$). **Right:** Stable invariant curve in the nonspatial matrix model with density-dependent maturation ($R = 70$). Solid lines are juveniles; dashed lines are adults. Circles indicate generations; connecting lines are for optical reasons only. In the right panel, the adult density is plotted at 20 times the actual density to make it visible on this scale. Parameters are $s_j = 0.5$, $s_a = 0.1$, and $g = 0.4$.

$$\mathbf{N}_{t+1}(x) = \int_{-L/2}^{L/2} \frac{a}{2} \exp(-a|x-y|) B(\mathbf{N}_t(y)) \mathbf{N}_t(y) \mathrm{d}y \,, \tag{13.25}$$

where $B(\mathbf{N})$ is the matrix in (13.23) but with the Ricker-type growth function $R\exp(-(J+A))$. We fix $L = 1$ and illustrate how the dynamics depend on the variance $\sigma^2 = 2/a^2$ of the dispersal kernel.

We fix parameters $s_j = 0.5$, $s_a = 0.1$, and $g = 0.4$. The critical value R^* for the nonspatial model to allow population persistence is $R^* \approx 3.15$. When $R^* < R < 14$, the nonspatial model has a unique stable persistence state. When $15 < R < 74$, we observe stable two-cycles, and for $74 < R < 100$ the system shows stable four-cycles; see left panel in Fig. 13.2.

As we turn to the spatial model, we fix $R = 80$. Then matrix B has the dominant eigenvalue $\mu_1 \approx 4.2012$. Since we fixed $L = 1$, we can solve relation (13.17) for dispersal parameter a and get a critical value of $a^* \approx 0.5697$, which translates into a critical variance of $(\sigma^2)^* \approx 6.1622$. When σ^2 is larger than this number, the zero state is stable and the population will not go extinct. As σ^2 decreases, the steady-state density increases; see top panels in Fig. 13.3. When $\sigma^2 < 4.5$, the steady state becomes unstable and a two-cycle emerges; see bottom left panel in Fig. 13.3. Finally, when $\sigma^2 = 0.05$, we even observe a four-cycle in the spatial model; see bottom right panel in Fig. 13.3.

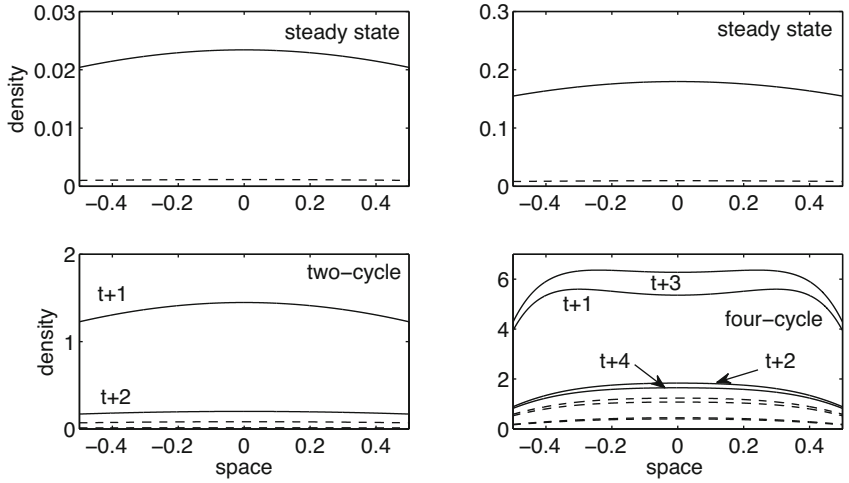

Fig. 13.3 Dynamics of the juvenile–adult model with density-dependent reproduction for different variances of the dispersal kernel. **Top left:** Stable persistence state for $\sigma^2 = 6$. **Top right:** Higher population densities at steady state with $\sigma^2 = 5$. **Bottom left:** Two-cycle for $\sigma^2 = 4$. **Bottom right:** Four-cycle for $\sigma^2 = 0.05$. For other parameters and details, see text. Solid lines represent juvenile densities; dashed lines represent adult densities.

Another interesting phenomenon arises when maturation instead of reproduction is density dependent (Neubert and Caswell 2000b). We keep R constant and replace g by $g\ \exp(-(J + A))$. Then the matrix and its limits at zero and at infinity are

$$B(\mathbf{N}) = \begin{bmatrix} s_j(1 - g\mathrm{e}^{-(J+A)}) & R \\ s_j g\mathrm{e}^{-(J+A)} & s_a \end{bmatrix}, \quad B(0) = \begin{bmatrix} s_j(1-g) & R \\ s_j g & s_a \end{bmatrix}, \quad B(\infty) = \begin{bmatrix} s_j & R \\ 0 & s_a \end{bmatrix}. \tag{13.26}$$

The eigenvalues of $B(0)$ are the same as in the previous scenario, and the eigenvalues of $B(\infty)$ are both less than unity. When $R^* < R < 49$, there is a globally stable positive state. When $R > 50$, however, this state is unstable and there is a stable oscillating solution; see right panel in Fig. 13.2. This solution seems to be periodic with period five, but it is not since we have a discrete-time system. Instead, the solution converges to the discrete-time analogue of a periodic orbit (an invariant closed curve). We will discuss this behavior in more detail at the beginning of Chap. 14.

We consider the effects of space on these dynamics in exactly the same setting as for Eq. (13.25) above: a one-dimensional habitat of length one and all dispersal kernels identical Laplace kernels. Since the linearization of this model is the same as above, the persistence condition is exactly as above. For $0.3 < \sigma^2 < 6.16$, we observe a stable persistence state. As we decrease the variance further, the persistence state becomes unstable and an oscillating solution appears. This solution seems very close to a period-four solution but is qualitatively very different from

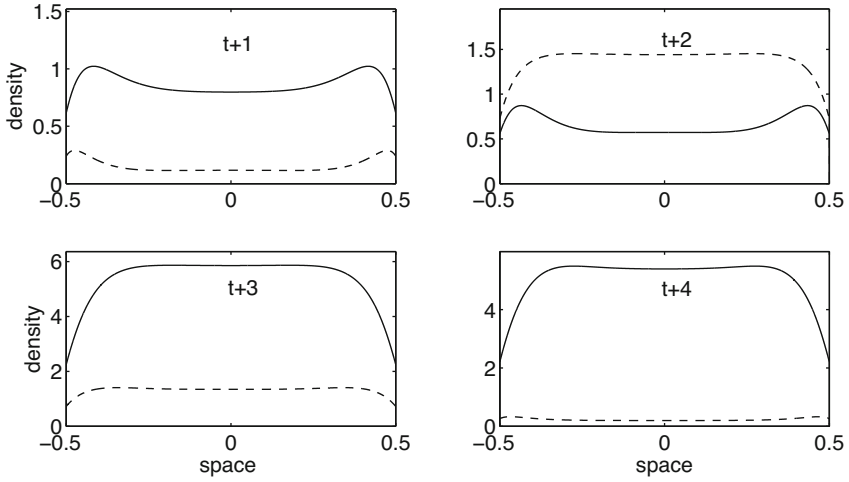

Fig. 13.4 Oscillatory dynamics of the juvenile–adult model with density-dependent maturation for $\sigma^2 = 0.01$. The four panels show the density of juveniles (solid) and the 20-fold density of adults (dashed) for four subsequent iterations after initial transients have disappeared. Subsequent iterations (modulo four) are indistinguishable from these four. Parameters are $s_j = 0.5$, $s_a = 0.1$, $g = 0.4$, $R = 80$, and $L = 1$.

the four-cycle that we observed in the previous scenario; see Fig. 13.4. Whereas the previous four-cycle had densities alternating between high and low from one generation to the next, this example shows two generations of high densities followed by two generations of low densities.

13.6 Traveling-Wave Speed in Unbounded Domains

When a population can persist locally, it is expected to spread spatially. We extend several ideas and results from the single-stage spread models in Chap. 5 to the stage-structured case. Not only is this theory well developed mathematically, it is also very widely and successfully applied to empirical data. We begin with a more heuristic approach to traveling-wave speeds and include a sensitivity analysis, which is useful and important in applications. We discuss the analysis behind the asymptotic spreading speed in Sect. 13.8.

Based on the approaches and results in Chap. 5, we assume that the dispersal kernels depend on distance only and are symmetric, i.e., $K(x, y) = K(|x - y|)$, and that vital rates are independent of spatial location. As before, we begin with the linear model, which we can consider as the linearization of (13.7) at the zero state. The equation reads

$$\mathbf{N}_{t+1}(x) = \int_{\mathbb{R}} [\mathbf{K}(x - y) \bullet B(0)]\mathbf{N}_t(y)\mathrm{d}y\,. \tag{13.27}$$

The traveling-wave ansatz $\mathbf{N}_t(x) = \mathbf{n}(\xi)$ with $\xi = x - ct$ and $c > 0$ leads to the relation

$$\mathbf{n}(\xi - c) = \int_{\mathbb{R}} [\mathbf{K}(\xi - \eta) \bullet B(0)]\mathbf{n}(\eta)\mathrm{d}\eta\,, \tag{13.28}$$

where $\eta = y - ct$. Since the equation is linear, we make the exponential ansatz

$$\mathbf{n}(\xi) = \mathrm{e}^{-s\xi}\phi\,, \tag{13.29}$$

where vector ϕ describes the relative abundances of the different stages in the traveling wave. Then we arrive at the eigenvalue equation

$$\mathrm{e}^{sc}\phi = \left[\int_{\mathbb{R}} \mathbf{K}(\nu)\mathrm{d}\nu \bullet B(0)\right]\phi = [\mathbf{M}(s) \bullet B(0)]\phi = \mathbf{H}(s)\phi\,, \tag{13.30}$$

where $\mathbf{M}$ denotes the matrix of moment-generating functions of the kernel matrix $\mathbf{K} = [k_{ij}]$ and $\mathbf{H}$ denotes the Hadamard product matrix. Alternatively, taking an exponential transform of (13.28) leads to the same result. Hence, we are looking for eigenvalues e^{sc} of matrix $\mathbf{H}(s)$.

Matrix $\mathbf{H}(s)$ has ℓ eigenvalues, denoted by $\lambda_i(s)$ with eigenvectors $\phi_i(s)$. By assumption, matrix $B(0)$ is nonnegative and primitive; by definition, $\mathbf{M}$ is positive. Therefore, $\mathbf{H}$ is nonnegative and primitive so that the Perron–Frobenius theorem applies. We denote by $\lambda_1(s)$ the dominant positive eigenvalue with positive eigenvector $\phi_1(s)$.

From any pair $\lambda_i(s)$, $\phi_i(s)$ we can form a solution of Eq. (13.27) as

$$\mathbf{N}_t(x) = \mathbf{n}(x - ct) = \mathrm{e}^{-s(x-ct)}\phi(s) = \lambda_i(s)^t\mathrm{e}^{-sx}\phi_i(s)\,. \tag{13.31}$$

Since the equation is linear, every linear combination of such solutions is again a solution. Dividing any linear combination

$$\mathbf{N}_t(x) = \sum_{i=1}^{\ell} \beta_i\lambda_i(s)^t\phi_i(s)\mathrm{e}^{-sx} \tag{13.32}$$

by the dominant eigenvalue, we find

$$\lim_{t\to\infty} \frac{\mathbf{N}_t(x)}{\lambda_1(s)^t} = \lim_{t\to\infty}\left[\beta_1\phi_1(s) + \sum_{i=2}^{\ell}\left(\frac{\lambda_i(s)}{\lambda_1(s)}\right)^t \beta_i\phi_i(s)\right]\mathrm{e}^{-sx} = \beta_1\phi_1(s)\mathrm{e}^{-sx}\,. \tag{13.33}$$

Since λ_1 is the dominant eigenvalue, all the fractions in the sum above converge to zero as $t \to \infty$.

We can then express the asymptotic speed of propagation via the dominant eigenvalue $\lambda_1(s)$ of $\mathbf{H}$ and the slope of the spatial decay as

$$c(s) = \frac{1}{s} \ln \lambda_1(s) . \tag{13.34}$$

This expression is the generalization of (5.16) to stage-structured models. In fact, in the case of a single stage, i.e., $\ell = 1$, matrix $\mathbf{H}$ reduces to a single element, which is also the "dominant eigenvalue," and which is given by $b_{11}M(s)$. This is exactly the expression in (5.16).

We have assumed that the population can persist locally; i.e., the dominant eigenvalue of $B(0)$ is greater than unity. We have further assumed that all dispersal kernels are symmetric, so that each element of $\mathbf{M}$ is bounded below by unity. Clearly, both matrices are nonnegative. Therefore, the dominant eigenvalue of $\mathbf{H}$ is also greater than unity. Hence, $c(s) > 0$ and the population can spread.

Now we consider the case where the vital rates are nonincreasing functions of density, i.e.,

$$B(\mathbf{N}) \leq B(0) . \tag{13.35}$$

Then any solution of the nonlinear IDE

$$\mathbf{N}_{t+1}(x) = \int_{\mathbb{R}} [\mathbf{K}(x-y) \bullet B(\mathbf{N}_t)]\mathbf{N}_t(y)\mathrm{d}y \tag{13.36}$$

is bounded by the solution of the linear equation in (13.27) with the same initial condition. Furthermore, if $\mathbf{N}_0(x) \leq \beta_1 \mathrm{e}^{-sx}\phi_1(s)$, then

$$\mathbf{N}_1(x) = \int_{\mathbb{R}} [\mathbf{K} \bullet B(0)]\mathbf{N}_0(y)\mathrm{d}y \leq \beta_1 \mathbf{H}(s)\phi_1(s)\mathrm{e}^{-sx} \tag{13.37}$$

$$\leq \beta_1 \lambda_1(s)\mathrm{e}^{-sx}\phi_1(s) = \beta_1 \mathrm{e}^{-s(x-c)}\phi_1(s) . \tag{13.38}$$

Iteratively, we can show the inequality

$$\mathbf{N}_t(x) \leq \beta_1 \mathrm{e}^{-s(x-ct)}\phi_1(s). \tag{13.39}$$

Finally, we note that any compactly supported initial condition can be bounded above by an exponential of the form $\beta_1 \mathrm{e}^{-sx}\phi_1(s)$ by choosing β_1 large enough for every s for which the moment-generating functions $\mathbf{K}$ exist. This reasoning proves the following lemma.

Lemma 13.6 *Assume that condition (13.35) holds. Then the spreading speed of the nonlinear model is bounded above by the minimal speed of traveling waves of the linearized equation, i.e., by*

$$\hat{c} = \inf_{s>0} \frac{1}{s} \ln \lambda_1(s) . \tag{13.40}$$

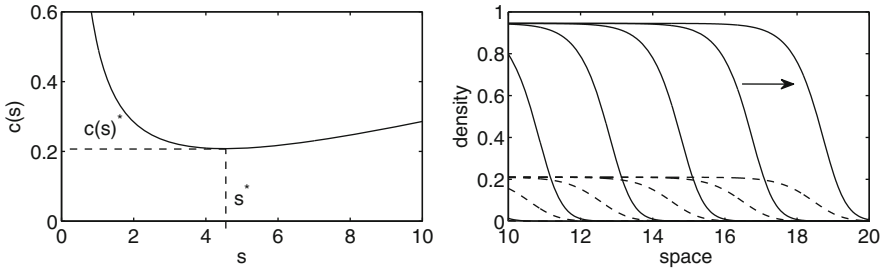

Fig. 13.5 **Left:** Dispersion relation $c(s)$ from (13.34) for the juvenile–adult model. Dashed lines indicate the minimum, $c(s^*)$, at s^*. **Right:** Advancing front of juveniles (solid) and adults (dashed) in the nonlinear model with density dependence in the growth rate. The density profile is plotted every 10 time steps. Parameters are $s_j = 0.5$, $s_a = 0.1$, $g = 0.4$, $R = 10$, and $\sigma^2 = 0.1$.

For an example, we return to the juvenile–adult model from Sect. 13.5. The matrix of vital rates is $B(0)$ as in (13.23). Let us consider a scenario where dispersal only happens at maturation and follows a Gaussian kernel with variance σ^2. None of the other stages disperses. Then the dispersal matrix is given by

$$\mathbf{K}(x) = \begin{bmatrix} \delta(x) & \delta(x) \\ \frac{1}{\sqrt{2\pi\sigma^2}} \exp(-\frac{x^2}{2\sigma^2}) & \delta(x) \end{bmatrix}. \tag{13.41}$$

We calculate

$$\mathbf{H}(s) = \begin{bmatrix} 1 & 1 \\ \exp(-\sigma^2 s^2/2) & 1 \end{bmatrix} \bullet \begin{bmatrix} s_j(1-g) & R \\ s_j g & s_a \end{bmatrix} = \begin{bmatrix} s_j(1-g) & R \\ s_j g \exp(\sigma^2 s^2/2) & s_a \end{bmatrix}. \tag{13.42}$$

The dominant eigenvalue of $\mathbf{H}(s)$ is

$$\lambda_1(s) = \frac{1}{2}\left(s_j(1-g) + s_a + \sqrt{(s_j(1-g) - s_a)^2 + 4 s_j g R \mathrm{e}^{\sigma^2 s^2/2}} \right). \tag{13.43}$$

We plot $c(s)$ in Fig. 13.5. With the chosen parameters, the minimum of $c(s)$ is $c^* = 0.208$ and occurs at $s^* = 4.53$. The dominant eigenvalue is $\lambda_1(s^*) = 2.56$, and a corresponding eigenvector is $\phi_1(s^*) = [1, 0.22]^T$.

To illustrate the advance of a traveling profile in the nonlinear equation, we let reproduction depend on density as in the previous section; i.e., we replace R by $R\exp(-J_t - A_t)$. We simulated the solutions of the IDE with initial conditions for juveniles and adults equal to 0.1 times the characteristic function of the negative half-line. Simulations develop the shape of the traveling profile after fewer than 10 iterations, and the distance per iteration is constant after 30 iterations. The resulting speed is $c = 0.198$, very close to the theoretically predicted value.

13.7 Sensitivity Analysis

As empirical measurements are always subject to various forms of error, we would like to know how the outcome of our calculations (here the minimal traveling-wave speed) depends on the input (here the parameters involved in our model). Answering this question is the goal of sensitivity analysis. *Sensitivity* measures the absolute change in the output quantity for a given change in the input quantity, whereas *elasticity* measures its relative change (Caswell 2001). In terms of the minimal traveling-wave speed $\hat{c} = c^*$ in (13.40) and some parameter p in the IDE, the two quantities are

$$\frac{\mathrm{d}c^*}{\mathrm{d}p} \qquad \text{and} \qquad \frac{p}{c^*}\frac{\mathrm{d}c^*}{\mathrm{d}p}\,, \tag{13.44}$$

respectively. The application of sensitivity analysis to spreading speeds in IDEs is developed by Neubert and Caswell (2000a).

Let p denote a parameter in IDE (13.27), either a population dynamic parameter in matrix $B(0)$ or a dispersal-related parameter in matrix $\mathbf{K}$. We consider the function of two variables

$$c(s, p) = \frac{1}{s}\ln(\lambda_1(s, p))\,. \tag{13.45}$$

We denote as $s^* = s^*(p)$ the value of s for which the minimum in (13.40) occurs, i.e., $c^*(p) = c(s^*(p), p)$. Then the sensitivity of c^* with respect to p is given by the chain rule as

$$\frac{\mathrm{d}c^*}{\mathrm{d}p} = \frac{\partial c}{\partial s}(s^*(p), p)\frac{\mathrm{d}s^*}{\mathrm{d}p}(p) + \frac{\partial c}{\partial p}(s^*(p), p)\,. \tag{13.46}$$

Since c^* is the minimum with respect to s, the first term on the right-hand side vanishes. Hence, we get

$$\frac{\mathrm{d}c^*}{\mathrm{d}p} = \frac{1}{s\lambda_1}\frac{\partial\lambda_1}{\partial p}\,. \tag{13.47}$$

In other words, the sensitivity of c^* is a multiple of the sensitivity of λ_1, the dominant eigenvalue of $\mathbf{H}$. Formulas for the sensitivity of an eigenvalue with respect to matrix entries h_{ij} are well known. They can be expressed in terms of the right and left eigenvectors ϕ_1 and ψ_1, respectively, as (Caswell 2001)

$$\frac{\partial\lambda_1}{\partial h_{ij}} = \frac{\psi_{1,i}\phi_{1,j}}{\langle\psi, \phi\rangle}\,, \tag{13.48}$$

where $\phi_{1,j}$ indicates the jth entry of vector ϕ_1. To find the sensitivity of c^* with respect to a parameter p that may appear in one or more entries h_{ij} of matrix $\mathbf{H}$, we use the chain rule again. We arrive at the following sensitivity formula.

Lemma 13.7 *The sensitivity of c^* with respect to some parameter p is given by the expression*

$$\frac{\mathrm{d}c^*}{\mathrm{d}p} = \frac{1}{s^*\lambda_1} \sum_{i,j} \frac{\partial \lambda_1}{\partial h_{ij}} \frac{\mathrm{d}h_{ij}}{\mathrm{d}p} = \frac{1}{s^*\lambda_1} \sum_{i,j} \frac{\psi_{1,i}\phi_{1,j}}{\langle \psi, \phi \rangle} \frac{\mathrm{d}h_{ij}}{\mathrm{d}p} \,. \tag{13.49}$$

We return to the example in Sect. 13.5 to illustrate these ideas. With parameters as in Fig. 13.5, we obtain $c^* = 0.208$ with $s^* = 4.53$ and $\lambda_1 = 2.56$. Matrix $\mathbf{H}$ and its eigenvectors are given by

$$\mathbf{H}(s^*) = \begin{bmatrix} 0.3 & 10 \\ 0.558 & 0.1 \end{bmatrix}, \quad \phi_1 = \begin{bmatrix} 0.9753 \\ 0.2208 \end{bmatrix}, \quad \text{and} \quad \psi_1 = \begin{bmatrix} 0.2393 \\ 0.9710 \end{bmatrix}. \tag{13.50}$$

We calculate

$$\frac{\mathrm{d}c^*}{\mathrm{d}R} = \frac{1}{s^*\lambda_1} \frac{\psi_{1,1}\phi_{1,2}}{\langle \psi, \phi \rangle} = 0.0102 \tag{13.51}$$

and

$$\frac{\mathrm{d}c^*}{\mathrm{d}\sigma^2} = \frac{1}{s^*\lambda_1} \frac{\psi_{1,2}\phi_{1,1}}{\langle \psi, \phi \rangle} \frac{s_j g s^{*2}}{2} \exp\left(\frac{\sigma^2 s^{*2}}{2}\right) = 1.04 \,. \tag{13.52}$$

Hence, an increase in R by a certain amount has a much smaller effect on c^* than an increase in σ^2 by the same amount. For example, increasing R from 10 to 10.1 and keeping all other parameters as in the previous example increases the speed from 0.208 to 0.209. Increasing σ^2 from 0.1 to 0.2, however, increases c^* to 0.29.

On the other hand, for the elasticities, we calculate

$$\frac{R}{c^*} \frac{\mathrm{d}c^*}{\mathrm{d}R} = 0.4887 \quad \text{and} \quad \frac{\sigma^2}{c^*} \frac{\mathrm{d}c^*}{\mathrm{d}\sigma^2} = 0.5014 \,. \tag{13.53}$$

Therefore, an increase of either R or σ^2 by the same percentage has almost the same effect on the speed. For example, increasing either R or σ^2 from the previous baseline values by 10% increases c^* to 0.2174 and 0.218, respectively. We illustrate these results in Fig. 13.6, where we plot the profile of juveniles after 80, 90, and 100 time steps from the same initial condition with different parameter values. The front with increased R is steeper and reaches a higher steady-state value but spreads at (almost) the same speed as the front for increased σ^2.

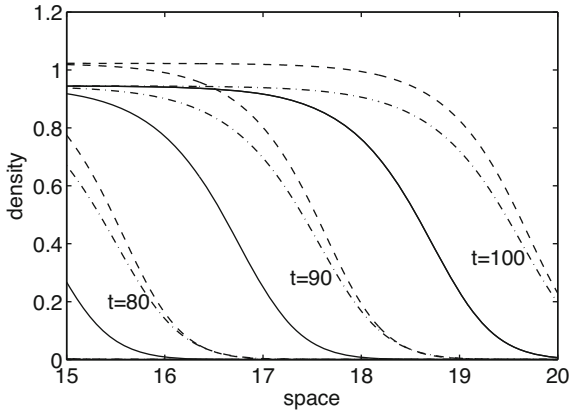

Fig. 13.6 Increasing parameter R or σ^2 in the juvenile–adult model with density-dependent reproduction increases the speed of spread. The density of juveniles is plotted after 80, 90, and 100 time steps, respectively, for baseline parameters from Fig. 13.5 (solid), increased reproductive rate (dashed), and increased variance of the Gaussian dispersal kernel (dash-dot). Increases are by 10%.

13.8 Spreading Speed for Structured Populations

Mathematically speaking, traveling waves are rather special solutions of IDEs. Their ecological interpretation is that the population is present in a very large region behind the invasion front. The asymptotic spreading speed (Definition 5.1) is a measure of the speed of propagation that is independent of the assumption of a traveling-wave profile. From an ecological point of view, it is more satisfying since it measures the spread of a population that is initially confined in space. From a mathematical point of view, this measure is more general than a traveling-wave speed but also more difficult to define and handle. In this section, we present the construction and basic concepts that lead to the definition of an asymptotic spreading speed as in Lui (1989a), but we refer to the original publication for the proofs. We consider the particular case of monostable dynamics on a one-dimensional domain; the general theory is given in Lui (1989a).

We study the recursion from (13.7) on the real line with spatially independent vital rates, so that the operator becomes

$$\mathbf{N}_{t+1} = \mathbf{Q}[\mathbf{N}_t] = \int_{\mathbb{R}} [\mathbf{K}(x-y) \bullet B(\mathbf{N}_t)]\mathbf{N}_t(y)\mathrm{d}y\,, \tag{13.54}$$

where $\mathbf{N} = [N^1, \ldots, N^\ell]^T$ as before. Throughout, we assume that B is nonnegative and primitive and that if $b_{ij} > 0$ for some $\mathbf{N} \geq 0$ then $b_{ij} > 0$ for all $\mathbf{N} \geq 0$. Whenever $b_{ij} > 0$, we also assume that the corresponding dispersal kernel $K_{ij} = K_{ij}(x-y)$ is a nonnegative symmetric bounded continuous function whose integral

over the entire real line is unity and whose moment-generating function exists. To define the most important property of $\mathbf{Q}$, we need to introduce an order structure on $\mathbb{R}^\ell$ and an appropriate function space.

For $\mathbf{n}, \mathbf{m} \in \mathbb{R}^\ell$, we define $\mathbf{n} \geq \mathbf{m}$ ($\mathbf{n} \gg \mathbf{m}$) if $n^i \geq m^i$ ($n^i > m^i$) for all $1 \leq i \leq \ell$. Furthermore, $\mathbf{n} > \mathbf{m}$ is a short notation for $\mathbf{n} \geq \mathbf{m}$ and $n^i > m^i$ for at least one i. The origin in $\mathbb{R}^\ell$ is denoted by $\mathbf{0}$. For a given vector $\mathbf{m} > \mathbf{0}$, we define the function space

$$\mathscr{C}_{\mathbf{m}} = \{\mathbf{N} \mid N^i : \mathbb{R} \to [0, m^i] \text{ piecewise continuous}^2\}. \tag{13.55}$$

We extend the order relation to $\mathscr{C}_{\mathbf{m}}$ by saying $\mathbf{N} \geq \widetilde{\mathbf{N}}$ ($\mathbf{N} \gg \widetilde{\mathbf{N}}$) if $\mathbf{N}(x) \geq \widetilde{\mathbf{N}}(x)$ ($\mathbf{N}(x) \gg \widetilde{\mathbf{N}}(x)$) for all $x \in \mathbb{R}$. We can always identify $\mathbf{n} \in \mathbb{R}^\ell$ with the constant function $N^i(x) = n^i$. By the assumptions on the dispersal kernels, if $\mathbf{n}$ is a constant function, then $\mathbf{Q}[\mathbf{n}]$ is also constant.

We now make assumptions on the local population dynamics that are closely related to those that led to the existence and uniqueness of a fixed point on a bounded domain in Sect. 13.4.

(S1) Function $\mathbf{N} \mapsto B(\mathbf{N})\mathbf{N}$ is nondecreasing for $\mathbf{N} \geq \mathbf{0}$.
(S2) There is a steady state $\mathbf{N}^* > \mathbf{0}$; i.e., $\mathbf{N}^* = B(\mathbf{N}^*)\mathbf{N}^*$.
(S3) For all initial conditions $\mathbf{n} \geq \mathbf{0}$ with $\mathbf{n} \neq \mathbf{0}$, the iteration $\mathbf{m}_{t+1} = B(\mathbf{m}_t)\mathbf{m}_t$ converges to $\mathbf{N}^*$.

With these assumptions, operator $\mathbf{Q}$ satisfies the following hypotheses from Lui (1989a):

1. $\mathbf{Q}: \mathscr{C}_{\mathbf{N}^*} \to \mathscr{C}_{\mathbf{N}^*}$, $\mathbf{Q}[\mathbf{0}] = \mathbf{0}$, $\mathbf{Q}[\mathbf{N}^*] = \mathbf{N}^*$.
2. $\mathbf{Q}$ commutes with translations; i.e., $\mathbf{Q}[\mathbf{N}(\cdot - y)](x) = \mathbf{Q}[\mathbf{N}](x - y)$.
3. $\mathbf{Q}$ is order preserving; i.e., if $\mathbf{N} \geq \widetilde{\mathbf{N}}$, then $\mathbf{Q}[\mathbf{N}] \geq \mathbf{Q}[\widetilde{\mathbf{N}}]$.
4. $\mathbf{Q}$ is continuous in the topology of uniform convergence on bounded subsets of $\mathbb{R}$.
5. For any $\mathbf{0} \ll \mathbf{n} \ll \mathbf{N}^*$, the iterates $\mathbf{Q}^{(k)}[\mathbf{n}]$ converge to $\mathbf{N}^*$ as $k \to \infty$.

Order-preserving operators have the following two important properties.

Lemma 13.8 (Proposition 2.1 in Lui 1989a)

1. *Let $\mathbf{R}_1$ or $\mathbf{R}_2$ be an order-preserving operator. Assume that sequences $\{\mathbf{n}_k\}$ and $\{\mathbf{m}_k\}$ satisfy $\mathbf{n}_{k+1} \geq \mathbf{R}_1[\mathbf{n}_k]$ and $\mathbf{m}_{k+1} \leq \mathbf{R}_2[\mathbf{m}_k]$, respectively. Suppose further that $\mathbf{R}_1[\mathbf{u}] \geq \mathbf{R}_2[\mathbf{u}]$ for all $\mathbf{u}$. If $\mathbf{n}_0 \geq \mathbf{m}_0$, then $\mathbf{n}_k \geq \mathbf{m}_k$ for all k.*
2. *Let $\mathbf{R}$ be an order-preserving operator. Assume that $\mathbf{R}[\mathbf{n}_0] \geq \mathbf{n}_0$ and define $\mathbf{n}_{k+1} = \mathbf{R}[\mathbf{n}_k]$. Then $\mathbf{n}_k$ is nondecreasing in k.*

[2] A function on some interval is *piecewise continuous* if the interval can be written as a finite number of subintervals such that the function is continuous on each open subinterval and has a finite limit at each endpoint of each subinterval.

We now present the construction that leads to the definition of the asymptotic spreading speed. We pick some vector $\mathbf{0} \ll \mathbf{m} \ll \mathbf{N}^*$ and continuous functions ϕ^i with the following properties:

1. $\phi^i : \mathbb{R} \to [0, m^i]$ is nonincreasing.
2. $\phi^i(s) = 0$ for $s \geq 0$.
3. $\phi^i(-\infty) = \lim_{s \to -\infty} \phi^i(s) = m^i$.

Then we define a sequence of functions $\mathbf{a}(c, \cdot)$ depending on a parameter c via

$$a_0^i(c, s) = \phi^i(s)\,, \tag{13.56}$$

$$a_{k+1}^i(c, s) = \max\{\phi^i(s), \mathbf{Q}[\mathbf{a}_k(c, \cdot + s + c)](0)\}\,. \tag{13.57}$$

The operator defined by the right-hand side of (13.57) is order preserving since $\mathbf{Q}$ is. The following properties of the sequence $\mathbf{a}_k$ are fairly straightforward to see.

Lemma 13.9 (Lemma 2.2 in Lui 1989a)

1. $\mathbf{a}_k(c, s)$ *is bounded between* $\mathbf{0}$ *and* $\mathbf{N}^*$.
2. $\mathbf{a}_k(c, s)$ *is nondecreasing in* k *and nonincreasing in* c *and* s.
3. $\mathbf{a}_k(c, -\infty)$ *exists, and* $\mathbf{a}_k(c, -\infty) \geq \mathbf{Q}^{(k)}[\mathbf{m}]$.
4. $\mathbf{a}_k(c, \infty) = 0$ *for all* k.
5. $\lim_{k \to \infty} \mathbf{a}_k(c, s) = \mathbf{a}(c, s)$ *exists and is nonincreasing in* c *and* s. *Furthermore,* $\mathbf{a}(c, -\infty) = \mathbf{N}^*$.

Before we define the asymptotic spreading speed, we give a rough illustration of the operator defined in (13.57). Let us consider the point $s = 0$ and some given element $\mathbf{a}_k$. Then the operator will first shift $\mathbf{a}_k$ to the left by c units; then apply the growth and dispersal operator $\mathbf{Q}$ to it, which presumably will help the species spread back to the right again; and then evaluate the result at $s = 0$. If the spreading to the right is in some sense "larger" than the shift by c to the left, then the value of $\mathbf{a}_{k+1}$ at $s = 0$ will be larger than that of $\mathbf{a}_k$ at $s = 0$; if it is smaller, then the reverse will happen. Hence, we could guess that for small enough values of c, the value of $\mathbf{a}_k(c, 0)$ will grow with k, but for large values it might not. We could therefore try to define the spreading speed as the value of c between these two scenarios. This idea can be used but we have to apply it at $s = \infty$ rather than $s = 0$.

We define

$$c^* := \sup\{c \mid \mathbf{a}(c, \infty) = \mathbf{N}^*\}\,. \tag{13.58}$$

Then the following can be shown.

Lemma 13.10 (Lemmas 2.4, 2.5, 2.6, and 2.9 in Lui 1989a)

1. $\mathbf{a}(c, s) \equiv \mathbf{N}^*$ *if and only if* $c < c^*$.
2. $\mathbf{a}(c, \infty)$ *is independent of the choice of* $\mathbf{m}$ *and* ϕ^i.
3. $\mathbf{a}(c, \infty) = \mathbf{Q}[\mathbf{a}(c, \infty)]$.
4. $\mathbf{a}(c, \infty) = \mathbf{0}$ *if* $c > c^*$.

We can now formulate the theorem that demonstrates that c^* is indeed the spreading speed of operator $\mathbf{Q}$; compare Chap. 5, Definition 5.1.

Theorem 13.3 (Theorems 3.1 and 3.2 and Proposition 3.3 in Lui 1989a) *Let (S1)–(S3) as well as the assumptions on* $\mathbf{K}$ *hold. Assume that* $\mathbf{Q}$ *is bounded above by its linearization at zero, i.e.,* $\mathbf{Q}[\mathbf{N}] \leq \mathbf{Q}'[0]\mathbf{N}$. *Assume furthermore that near zero,* $\mathbf{Q}$ *can be bounded below, e.g.,* $\mathbf{Q}[\mathbf{N}] \geq (1-\epsilon)\mathbf{Q}'[0]\mathbf{N}$ *for* $\|\mathbf{N}\|$ *small enough. Pick* $\mathbf{0} \neq \mathbf{N}_0 \in \mathscr{C}_{\mathbf{N}^*}$ *with compact support and define* $\{\mathbf{N}_t\}$ *through the recursion (13.54). Then the following hold for any small* $\epsilon > 0$:

$$\limsup_{t\to\infty} \max_{|x|>(c^*+\epsilon)t} \mathbf{N}_t(x) = \mathbf{0}\,,$$

$$\liminf_{t\to\infty} \min_{|x|<(c^*-\epsilon)t} \mathbf{N}_t(x) = \mathbf{N}^*\,.$$

Finally, Theorems 3.4 and 3.5 in Lui (1989a) guarantee that the spreading speed defined in (13.58) can be calculated by the formula in (13.40).

The original results by Lui (1989a) require that the initial condition is sufficiently large on a sufficiently large domain. When there is no Allee effect in the IDE, the "hairtrigger effect" (Weinberger 1982) ensures that any nonnegative, nonzero initial condition will eventually meet these requirements. The original results also require the kernels to have compact support. This requirement is removed by Liang and Zhao (2007). The theory formulated by Lui (1989a) and earlier for the scalar case by Weinberger (1982) is substantially more general than the version presented here. We mention a few aspects. First, the formulation by Lui (1989a) is based on some abstract operator $\mathbf{Q}$ and its properties. The theory is well suited to applications to IDEs, as we saw, but not limited to those. For example, it also applies to a time-one map of (systems of) reaction–diffusion equations. The abstract theory has since been developed significantly further by several authors, e.g., Liang and Zhao (2010). Second, the work in Lui (1989a) does not address the question of the existence of traveling waves treated in the scalar case by Weinberger (1982), but many authors since then have worked on this problem. A survey on the theory of spreading speeds and traveling waves for monotone systems of equations can be found in Zhao (2009). Third, the formulation by Lui (1989a) includes the case of an Allee effect, which we excluded here in assumption (S3). As we have seen in Chap. 6, the elegant spread speed formula (13.40) cannot be expected to hold in the presence of an Allee effect. The asymptotic speed of spread still exists, but it may be negative and, most important, for a population to actually spread at this speed, its initial density has to be high enough over a large enough set. For details, see Theorems 3.1 and 3.2 in Lui (1989a). Finally, the general theory is formulated for spreading phenomena in several spatial dimensions and not only one-dimensional space as presented here. We then formulate a spreading speed in a given direction and consider planar traveling waves in that direction. Amor and Fort (2009) formulate an explicit two-dimensional model, derive the corresponding formula for the spreading speed based on the linear conjecture, and compare how one- and two-dimensional structured and unstructured spread rates differ.

13.9 Further Reading

The aspects of IDEs for stage-structured populations presented in this chapter are only the basics of the existing theory. Because these structured equations can describe such rich life histories, the number of modifications and interesting questions seems almost infinite. The following summaries are meant to point the interested reader to the existing body of literature.

Dynamics on Bounded Domains

Fagan and Lutscher (2006) apply the theory by Lutscher and Lewis (2004) to a two-stage model of swift fox (*Vulpes velox*) population dynamics to estimate the habitat size required for conservation of the species. This application includes the scenario that the bounded domain consists of two disjoint subdomains corresponding to two spatially separated patches of habitat. We will investigate these ideas further in Chap. 15 when we focus on ways to include spatial variation in IDE models.

A bifurcation theory for systems of IDEs, somewhat more abstract than the results presented here, is developed independently in Alzoubi (2007, 2010a,b). It is based on the general theory of global bifurcations by Rabinovitz. Another series of papers uses the same bifurcation-theoretic approach—in addition to numerical experiments—and expands the problems studied via IDEs in various directions (Robertson 2009; Robertson and Cushing 2011, 2012; Robertson et al. 2012). The authors study the question of spatial segregation between life stages in a flour beetle population in a homogeneous habitat. They propose a dispersal kernel very different from the kernels presented here so far. In their approach, the probability that an individual will move to a certain location depends only on that location and not on the individual's initial location. This approach implies that the domain is relatively small compared to the individual's dispersal ability, so that individuals can reach any location from any point within a single dispersal period. Furthermore, the authors assume that dispersal is density dependent so that the probability of moving to a certain location decreases with the density of individuals already there. For an example with juveniles and adults, the authors choose

$$K(x, y, J, A) = \frac{1}{2}\sin(x)\exp(-D(s_j J(x) + s_a A(x)) \tag{13.59}$$

on the domain $\Omega = [0, \pi]$. When $D = 0$, dispersal is density independent. Increasing parameter D leads to avoidance of areas where the density is high. It would be an interesting challenge to derive dispersal kernels for avoidance (or attraction) from mechanistic random-walk models in the spirit of Chap. 7.

When the life cycle of an organism consists of many stages, it is typical for dispersal to be limited to only a few stages or transitions between stages, as discussed in Sect. 12.4. Formulating a model with nondispersing stages is fairly

simple: the corresponding dispersal kernel is a delta distribution; see, e.g., matrix **K** in (13.41). Analyzing the dynamic behavior when there are sedentary stages is much harder. The mathematical reason for this difficulty is that the operators involved fail to be compact, whereas many of the existing theorems about stability and bifurcation require compactness. Corresponding results about critical patch-size and existence of steady states can still be achieved in several cases. For example, operator **Q** in (13.7) may not be compact but some iterate of it is compact if individuals have to go through a dispersal stage after finitely many generations. In that case, we can apply the theory to the corresponding power of **Q**. Alternatively, we can sometimes decompose the operator into the sum of a compact and a nilpotent operator and obtain the desired results. Details of these two approaches are laid out in Lutscher and Lewis (2004). Jin et al. (2016) develop a general theory for population persistence and extinction when the next-generation operator can be written as the sum of a contraction and a compact operator. This theory applies to the structured population models studied here, provided that certain conditions hold. In particular, if we write **Q** as a sum of those transitions relating to reproduction and those that relate to survival, then the part that relates to survival only is a contraction. If all components of the part with reproduction disperse, then that part of the operator is compact.

Spread on Unbounded Domains

We need to formulate stage-structured models because for many species, individuals of different life-history stages exist simultaneously. The stage-structured model projects the densities of all stages per year or some other suitable time unit. It takes several of these time units to complete a generation. Bateman et al. (2015) introduce the concept of a "generational spreading speed," the distance that a population front covers from one generation to the next. The methods are similar to the ones introduced above, but the authors use graph reduction techniques to simplify the full annual stage-structure dynamics to generational dynamics.

One of the biggest challenges for the mathematical theory of spread on unbounded domains is the loss of compactness of the operator **Q** in model (13.54) when some of the dispersal kernels are delta distributions. While the asymptotic spreading speed can still be defined and can be shown to exist, including the formula from the linearization, the proof of existence of a traveling wave in Weinberger (1982) relies on a compactness argument. One way to prove the existence of traveling waves is to decompose the operator into a compact operator and a contraction if the model structure allows it. This idea is developed by Le et al. (2011) and Lutscher and Van Minh (2013).

An abstract, very general theory of spreading speeds and traveling waves in Banach lattices is developed by Liang and Zhao (2010). The authors replace the requirement of compactness by the requirement that operator **Q** decrease the Kuratowski measure of noncompactness of a set. This theory applies to a wide range

of types of equations, not only IDEs. Fang and Zhao (2014) use an even weaker compactness assumption but apply their theory to continuous-time equations only. A more direct approach for IDEs is carried out by Meyer (2012) and Meyer and Li (2013). These authors derive a structured IDE with infinitely many stages. Their model is motivated by a plant species with a seed bank where seeds can lie dormant for arbitrarily long times. They prove the existence of a spreading speed and of traveling waves for their model. They also prove the usefulness of the linearization formula and they consider nonmonotone growth functions. An earlier model with infinitely many stages in a completely different context was derived by Powell et al. (2005); see below.

In some cases, a scalar IDE may contain a time delay; i.e., the density at time $t + 1$ is determined by the density not only at time t but also at previous times. Accordingly, operator Q may depend on $N_t, N_{t-1}, \ldots$. Such equations may be reformulated as a structured model with nondispersing stages, and the existence of spreading speeds and traveling waves may be proved in that setting (Lin and Li 2010). These authors also show the stability of the traveling-wave front.

Another dimension for structuring a population is sex. If males and females have significantly different dispersal behavior, then distinguishing between them could be important for correctly predicting population spread rates. Miller et al. (2011) formulate and analyze the first two-sex model for invasions. They derive a heuristic formula for the spreading speed and use numerical simulations to demonstrate its validity, but a mathematical proof of its correctness is still missing.

Disease stage may constitute yet another factor of the structure of a population. For example, Marculis and Lui (2015) formulate a model for green crab with a juvenile, a susceptible-adult, and an infected-adult stage. The most interesting aspect of this model in the present context is that there can be a semi-trivial boundary state where some stages are positive (e.g., juveniles and susceptible adults), whereas others are zero (e.g., infected adults). The existence of a semi-trivial boundary stage violates the assumption made by Lui (1989a) that there be a unique positive equilibrium. Numerical simulations by Marculis and Lui (2015) reveal that the equations may support *stacked waves*: a traveling wave that connects the zero state with the semi-trivial boundary state and a secondary wave that connects that boundary state with the positive stage. The phenomenon is closely related to the observation of traveling two-cycles in Sect. 11.4. The analysis of such stacked waves is still wide open. Bateman et al. (2017) provide more simulation results on stacked waves in a closely related model for green crab with a castrating parasite.

Applications to Spread and Biological Invasions

We need to formulate stage-structured models because for many species, individuals of different life history stages exist simultaneously. There are, however, other scenarios to which this theory applies. For example, Lui (1989b) calculates spread rates for a population genetics model with equations for allele frequencies in the

female and male subpopulation. He also applies the theory to an epidemic model that tracks the progression of a disease between a host and a vector.

A stage-structured model projects the densities of all stages per year or some other suitable time unit. It takes several of these time units to complete a generation. Bateman et al. (2015) introduce the concept of a "generational spreading speed," the distance that a population front covers from one generation to the next. The methods are similar to the ones introduced above, but the authors use graph reduction techniques to simplify the full annual stage-structured dynamics to generational dynamics.

Neubert and Caswell (2000a) develop the theory and apply it to two herbaceous flowering plants with six (*Dipsacus sylvestris*) and eight (*Calathea ovandensis*) stages. Among other things, the authors find that the speed of spread is highly sensitive to long-distance dispersal, a phenomenon that we discussed in Sect. 12.5. Caswell et al. (2003) expand the theory to use order statistics to calculate sensitivities and apply the techniques to three bird species with three stages each, namely Pied Flycatcher (*Ficedula hypoleuca*), Starling (*Sturnus vulgaris*), and Sparrowhawk (*Accipiter nisus*). Neubert and Parker (2004) review the calculation of spread rates and sensitivity analysis of IDEs for risk analysis of invasive species and apply it to scotch broom.

Le Corff and Horvitz (2005) use a stage-structured IDE to study the effects on population spread of the mixed reproductive strategy of a tropical herb (*Calathea micans*) with obligate selfed or potentially outcrossed seeds and dispersal by ants.

Jacquemyn et al. (2005) study the spread of perennial tussock grass *Molinia caerulea* in a heathland, in particular the effect of fire on the success of this invasive heathland plant.

Buckley et al. (2005) develop a stage-structured model for a pine invasion in New Zealand. They represent long- and short-distance dispersal by a mixed dispersal kernel consisting of a Laplace and a Gaussian kernel. Based on sensitivity analysis, they give some management recommendations on how to slow the invasion.

Vellend et al. (2006) consider the dual effect of herbivores on the spread of the forest herb *Trillium grandiflorum*: deer consume the plant and thereby inhibit its growth, but they also transport its seed and thereby facilitate its spread. Their seven-stage IDE model illustrates how the additional dispersal mechanisms outweigh the negative effects on population growth at low levels of herbivory and can explain range expansion of the herb at the northern edge of its range.

Garnier and Lecomte (2006) use a stage-structured model for transgenic oilseed rape with a combination of dispersal kernels accounting for long- and short-distance dispersal to estimate the spread risk of feral plants. Garnier et al. (2008) measure probabilities and distances of roadside spread and include them into their previous model.

Jongejans et al. (2008) use a four-stage model of the thistle (*Carduus nutans*) and develop a variance-decomposition method to study the relative impact of population dynamics and dispersal mechanisms. They employ the WALD model to generate dispersal kernels that include a distribution of seed release height and hourly wind-speed data. In a later investigation of the same species, Shea et al. (2010) study

several management options by comparing sensitivities of the spread rate with respect to parameters in three different environments, one native and two invaded. Zhang et al. (2011) follow up on this study by exploring how global warming can speed up invasions of this thistle. Caplat et al. (2012) also use the WALD model to generate a dispersal kernel, and they apply it to the invasion of Corsican pine in New Zealand. Caplat and Buckley (2012), based on Buckley et al. (2005), present a more general article on management applications of structured IDEs.

Soons and Bullock (2008) generate dispersal kernels from wind tunnel experiments and wind speeds measured in the field. They study in particular the effect of nonrandom seed release in two heathland plants, *Calluna vulgaris* and *Erica cinerea*. These plants release their seeds only when wind speeds exceed a certain threshold, and in particular during wind gusts. This mechanism leads to predicted wave speeds that are twice as high as with temporally random seed release.

Bullock et al. (2008) consider a stage-structured IDE for the rare annual herb *Rhinanthus minor* under four different management options (grazing versus cutting) and calculate corresponding spread rates.

Miller and Tenhumberg (2010) study the spread of the Diaprepes root weevil (*Diaprepes abbreviatus*) in Florida with a six-stage IDE. They find, among other things, that transient speeds of range expansion at the onset of an invasion can be higher than the asymptotic speed, and that measures to reduce the asymptotic speed may have little or no effect on transient speeds.

Gruess et al. (2011) formulate a two-stage IDE to evaluate the relative impacts of adult movement and juvenile dispersal, as well as harvesting, on the effectiveness of marine reserve networks.

Travis et al. (2011) compare analytical predictions of a stage-structured IDE with simulation results from an individual-based model for the invasive shrub *Rhododendron ponticum*. They argue in particular that the two modeling approaches should be seen as complementary and used in conjunction since each can inform the other.

Bullock et al. (2012) use climate modeling and the WALD model to predict future wind speeds and their variation. They then include this information in mechanistic dispersal kernels and predict the ability of wind-dispersed plants to keep up with climate change; see Sect. 12.3.

Matlaga and Davis (2013) use a stage-structured IDE model to estimate the invasive potential of the engineered bioenergy crop *Miscanthus* $\times$ *giganteus*.

Lamoureaux et al. (2015) consider a seven-stage IDE for the weedy grass *Nassella trichotoma* to evaluate the need for and cost effectiveness of various control strategies of this plant.

Structured IDEs are also used to model species spread and invasions in advective environments with asymmetric dispersal. Pringle et al. (2009) generalize some of the ideas from Sect. 12.2 to structured populations; in particular, they characterize the critical population growth rate for persistence under biased dispersal. Gharouni et al. (2015) derive a three-stage model for a green crab invasion with biased dispersal. Krkošek et al. (2007) fit several dispersal kernels to the northern and southern spread of sea otters in California. They find that heavy-tailed dispersal kernels that predict

accelerating invasions fit the observations very well. Smith et al. (2009) reanalyze the sea otter data but introduce spatial heterogeneity by assuming that population vital rates differ between the northern and southern directions.

A series of papers develops models and fits data of the spread of the late blight disease in potatoes and tomatoes and its pathogen *Phytophthora infestans*. The quantity of interest is the density of lesions caused by the pathogen. These lesions are structured by age, and their area increases with age. Lesions "disperse" through spores that are moved by wind or splatter with rain drops. The model development with infinitely many stages is presented by Powell et al. (2005). Several other papers are parameterized by field experiments and study the effect of host plant diversity, spatial scale of heterogeneity, and weather (Skelsey et al. 2005, 2009a,b, 2010).

On a much larger scale, Heavilin and Powell (2008) model the spread of pine tree (*Pinus contorta* Douglas) death due to attacks from mountain pine beetle. They structure trees as juvenile (which are not susceptible), susceptible, and infected. Infections spread through beetle reproduction and flight. This model exhibits an Allee effect, as a susceptible tree can fend off a small enough number of beetles. The authors then obtain parameter estimates through a maximum likelihood procedure.